



## **Effective Rejection of Fluorescence Interference in Raman Spectroscopy Using a Shifted Excitation Difference Technique**

**ANDREW P. SHREVE,  
NERINE J. CHEREPY, and  
RICHARD A. MATHIES\***

*Department of Chemistry, University of California,  
Berkeley, California 94720*

**Index Headings:** Raman spectroscopy; Fluorescence rejection; Wavelength modulation; CCD detectors; Multichannel difference spectroscopy; Spectroscopic techniques.

### **INTRODUCTION**

Resonance Raman spectroscopy is a powerful technique for probing the vibrations of particular chromophores in multicomponent systems. By tuning the wavelength of the excitation laser into resonance with an electronic absorption band of only one molecular species, the vibrational Raman scattering from this species can be selectively enhanced. Thus, resonance Raman spectroscopy can provide structural information for chromophores in solution or biological chromophores within their functionally active protein environment. However, since the very nature of the experiment requires that the excitation light be absorbed by the sample, the measurement of resonance Raman spectra is often made difficult by a large fluorescence background in the same spectral region as the Raman scattering. The problem of fluorescence interference from intrinsic sample emission is often further exacerbated in biological samples, where low-concentration impurities with large fluorescence yields can be difficult to remove. Even weak fluorescence, with an effective fluorescence quantum yield of  $\approx 10^{-4}$ , completely overwhelms resonance Raman signals, which have typical quantum yields of  $\approx 10^{-7}$ .

Many techniques have been used to discriminate against the fluorescence background in spontaneous Raman experiments.<sup>1-20</sup> One simple approach is to add a

fluorescence quencher.<sup>1</sup> However, in this technique the sample must be unperturbed by the addition of a fluorescence quencher in high concentrations—a condition that is often not satisfied for biological samples. Another approach is to excite the sample with the use of a wavelength that is longer than the lowest energy absorption band (pre-resonance excitation).<sup>2-5</sup> An important technique exploiting this idea is Fourier transform (FT) Raman spectroscopy.<sup>2,3</sup> In many cases Raman spectra of highly fluorescent chromophores can be obtained in this manner; however, there are some serious limitations. First, the excitation is not directly on resonance with any chromophore, so in a system with multiple chromophores, selective enhancement of Raman scattering will not occur. Second, since the excitation is limited to pre-resonance wavelengths, resonance Raman excitation profiles (Raman intensity as a function of excitation wavelength) cannot be measured through the absorption band. This is a serious drawback since the analysis of excitation profiles is quite useful for probing the properties of a chromophore's excited electronic states.<sup>21</sup>

In some cases the Raman scattering and fluorescence emission can be distinguished temporally.<sup>6-12</sup> If the fluorescence emission is from an electronic state whose lifetime is long relative to the laser pulse duration and the detection time, then one can simply subtract the spectrum observed with a detection time gate set after the end of the laser pulse (pure fluorescence) from the spectrum observed with a detection time gate coincident with the laser pulse (both Raman and fluorescence). Schemes that are based upon this idea but use either gated or time-correlated photon counting to provide time resolution have also been developed.<sup>6-9,11,12</sup> A different approach to time-based fluorescence rejection involves high-frequency modulation of the laser intensity, either by mode-locking the laser<sup>13</sup> or by using a modulator external to the cavity.<sup>14,15</sup> If the fluorescence has a characteristic decay time longer than the period of the modulation, then the fluorescence is demodulated, while the Raman signal, of course, faithfully follows the modulation of the excitation laser. Thus, if the combined Raman and fluorescence are passed through an electro-optic demodulator prior to detection,<sup>15</sup> or if they are detected with a spectrum analyzer<sup>13</sup> or a phase-sensitive lock-in apparatus,<sup>14</sup> then the fluorescence background can be rejected.

Another scheme for distinguishing Raman scattering from fluorescence involves wavelength modulation of the excitation laser.<sup>16-20</sup> In the past, this technique has been implemented by introducing a low-frequency modulator

Received 4 November 1991.

\* Author to whom correspondence should be sent.

into the tuning element of a cw dye laser. The Raman peaks track with the wavelength of the laser, but the fluorescence is nearly unchanged by a small change in excitation wavelength. Thus, if the dispersed Raman and fluorescence are observed with the use of a lock-in detection apparatus, a derivative Raman spectrum, essentially background free, can be obtained.

While the fluorescence rejection techniques described above have seen some use, their applicability is somewhat limited. The time-based techniques (including intensity modulation techniques) are useful only if the fluorescence is relatively long lived. While this is often true if the interfering fluorescence is from an impurity or if the emitting state is not reactive, in many cases the fluorescence is intrinsic emission from a short-lived, chemically reactive state. Examples of systems where time-based fluorescence rejection techniques will not work are the proteins bacteriorhodopsin and bacterial photosynthetic reaction centers, both of which have intrinsic fluorescence yields for  $S_1 \rightarrow S_0$  emission of  $\approx 10^{-4}$ , but fluorescence lifetimes on the order of  $10^{-12}$  seconds. Wavelength modulation techniques can be applied to any system, but their use seems to have been limited by the need for specialized equipment for low-frequency modulation of the laser wavelength and for lock-in detection. In addition, lock-in detection precludes the use of multichannel detectors, such as a diode array or a charge-coupled device (CCD), for viewing the spectrally dispersed Raman signal. Because single-channel detection requires much longer signal accumulation times, this is a serious concern for Raman experiments on difficult-to-prepare samples that are photochemically labile—a situation often encountered in Raman spectroscopy of biological systems.

In this paper we describe a simple fluorescence rejection technique, shifted excitation Raman difference spectroscopy (SERDS), based on taking the difference of two spectra obtained with slightly shifted excitation frequencies. While this approach is conceptually similar to previous wavelength modulation techniques,<sup>16–20</sup> our method offers the following improvements: First, in contrast to the previous techniques, no special equipment is required for changing the wavelength of the excitation laser. Second, multichannel detection is used, resulting in improved signal-to-noise for a given accumulation time. With modern, cooled, unintensified CCD detectors the very high, shot-noise-limited, signal-to-noise ratio that is critical for such differencing methods can be achieved easily (for a recent review of CCDs, see Epperson *et al.*<sup>22</sup>). In addition to these features, the method is equally applicable to samples with either short-lived or long-lived fluorescence interference.

## EXPERIMENTAL

In order to characterize the shifted excitation difference method, we have examined Raman scattering from chloroform ( $\text{CHCl}_3$ ) with various amounts of laser dye added to simulate fluorescent impurities. Spectral-grade  $\text{CHCl}_3$  was used without further purification, and the laser dye LDS-925 was used as obtained from Exciton Chemical.

The excitation source was a Lexel Ti:sapphire laser (Model 479) pumped by a Spectra-Physics Ar<sup>+</sup> laser

(Model 2020) running all lines. The Ti:sapphire output was directed through an Amici prism to eliminate spontaneous emission and then focused into the sample using a spherical lens of 75 mm focal length. Typical excitation powers were 3 mW, and the illuminated area at the sample was  $\approx 10^{-4} \text{ cm}^2$ . The magnitude of both the Raman lines of the solvent and the fluorescence background was found to depend linearly upon excitation power at the energies used. The sample was circulated at low speed through a 1-mm-i.d. square glass capillary to eliminate long-time photobleaching, and the combined Raman scattering and fluorescence emission were collected with a standard 90° arrangement. The collected light was imaged with  $7\times$  magnification onto the entrance slit of a  $\frac{3}{4}$ -meter double spectrograph modified to run in an additive-subtractive dispersive mode.<sup>23</sup> With the use of a 600 line/mm grating in the first stage in +1st order and a 1200 line/mm grating in the second stage in –1st order, for 775 nm excitation approximately  $550 \text{ cm}^{-1}$  ( $\approx 35 \text{ nm}$ ) of the dispersed spectra was imaged onto a CCD detector (Princeton Instruments, Model LN-CCD). The detector, operated at  $-100^\circ\text{C}$ , was equipped with an EEV Model 88130 array with an active area of  $6.7 \times 26 \text{ mm}$  and a 16-bit A/D converter. For all data reported here, the total exposure time for each spectrum was six minutes.

To obtain a shifted excitation difference spectrum, one uses the following procedure: First, the spectrum,  $S_a(\bar{\nu})$ , of the combined fluorescence emission and Raman scattering is measured with excitation frequency  $\bar{\nu}_a$ . Then, with the birefringent tuning element of the Ti:sapphire laser, the excitation frequency is changed to  $\bar{\nu}_b = \bar{\nu}_a + \delta$  and another spectrum,  $S_b(\bar{\nu})$ , is obtained with all other conditions unchanged. The difference of these spectra,  $S(\bar{\nu}) = S_b(\bar{\nu}) - S_a(\bar{\nu})$ , is then computed. Because the fluorescence is essentially unaffected by the shift in excitation frequencies, the fluorescence background in the difference spectrum is nearly absent (a small difference from zero is sometimes observed in  $S(\bar{\nu})$ , possibly because of the presence of some unrelaxed fluorescence). In contrast, the Raman peaks shift with the excitation frequency, so Raman scattering appears as derivative-shaped features in  $S(\bar{\nu})$ . In order to generate a conventional Raman spectrum from the difference spectrum, the difference spectrum is modeled. Though more complicated models are also easy to implement,<sup>24</sup> we have chosen to use a simple one that assumes the original Raman spectrum,  $R(\bar{\nu})$ , to consist of  $N$  Gaussian peaks,

$$R(\bar{\nu}) = \frac{1}{\sqrt{2\pi}} \sum_{i=1}^N \frac{A_i}{\sigma_i} \exp \left[ -\frac{(\bar{\nu} - \bar{\nu}_{0i})^2}{2\sigma_i^2} \right]. \quad (1)$$

Then the difference spectrum (shifted minus unshifted) is

$$S(\bar{\nu}) = \frac{1}{\sqrt{2\pi}} \sum_{i=1}^N \frac{A_i}{\sigma_i} \left\{ \exp \left[ -\frac{(\bar{\nu} - \bar{\nu}_{0i} + \delta)^2}{2\sigma_i^2} \right] - \exp \left[ -\frac{(\bar{\nu} - \bar{\nu}_{0i})^2}{2\sigma_i^2} \right] \right\}. \quad (2)$$

Each peak  $i$  is characterized by an area  $A_i$ , a center position  $\bar{\nu}_{0i}$ , and a standard deviation  $\sigma_i$ . Equation 2 is used to fit the measured difference spectrum using a Marquardt nonlinear least-squares fitting routine. The pa-

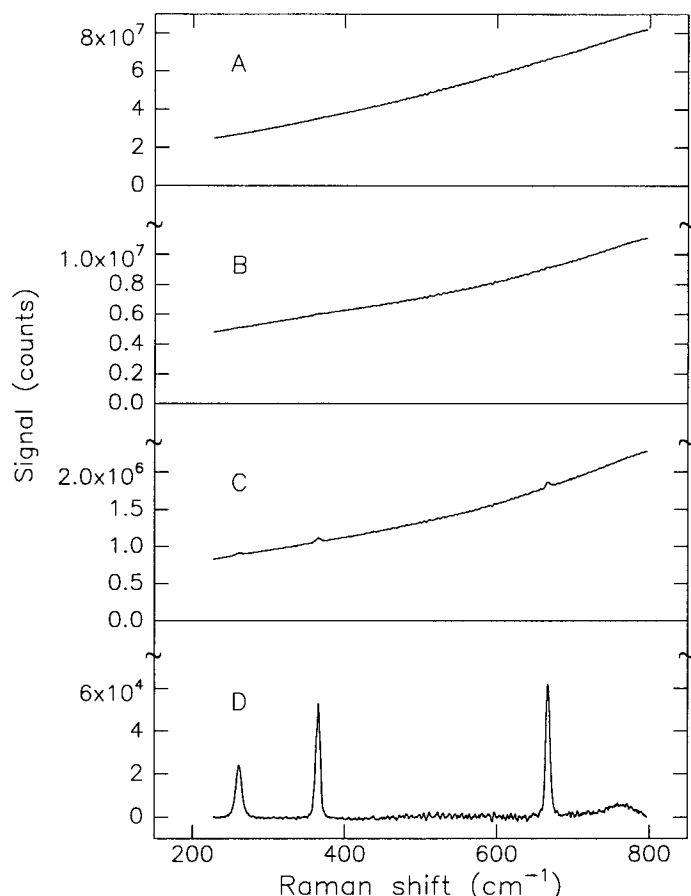


FIG. 1. Emission spectra, obtained with 3 mW of 775 nm exciting light, of a series of  $\text{CHCl}_3$  solutions with varying amounts of LDS-925 added. (A)  $\approx 4 \times 10^{-5}$  M LDS-925 in  $\text{CHCl}_3$ ; (B)  $\approx 6 \times 10^{-6}$  M LDS-925 in  $\text{CHCl}_3$ ; (C)  $\approx 1 \times 10^{-6}$  M LDS-925 in  $\text{CHCl}_3$ ; (D) neat  $\text{CHCl}_3$ . Note the different vertical scales for each panel. All spectra are corrected for the wavelength sensitivity of the instrument response. The entrance slit of the spectrograph was set to yield  $7 \text{ cm}^{-1}$  resolution at 775 nm, and the accumulation time for each spectrum was 6 min.

rameters obtained are then used in Eq. 1 to generate  $R(\bar{\nu})$ .

## RESULTS AND DISCUSSION

The Raman spectra of neat  $\text{CHCl}_3$  and  $\text{CHCl}_3$  with various amounts of added LDS-925 are shown in Fig. 1. The unshifted excitation wavelength for these, and all other data, was 775 nm. The Raman spectrum of pure  $\text{CHCl}_3$  is shown in panel D. At the lowest concentration of added dye (panel C), which raises the fluorescence background to  $\approx 30$  times the Raman intensity, the strong  $\text{CHCl}_3$  Raman lines at 262, 366, and  $668 \text{ cm}^{-1}$  can still be observed. In this case the removal of the fluorescence background by a simple background subtraction using either a spline or polynomial fit to the background would be possible. In contrast, for the data shown in panels B and A, the increasingly larger fluorescence background completely obscures the Raman lines of the solvent. Under such conditions an attempt to obtain the Raman spectrum by subtraction of a fit to the fluorescence background, particularly if the positions of the Raman lines were previously unknown, would yield uncertain results.

In Fig. 2, shifted excitation difference spectroscopy is

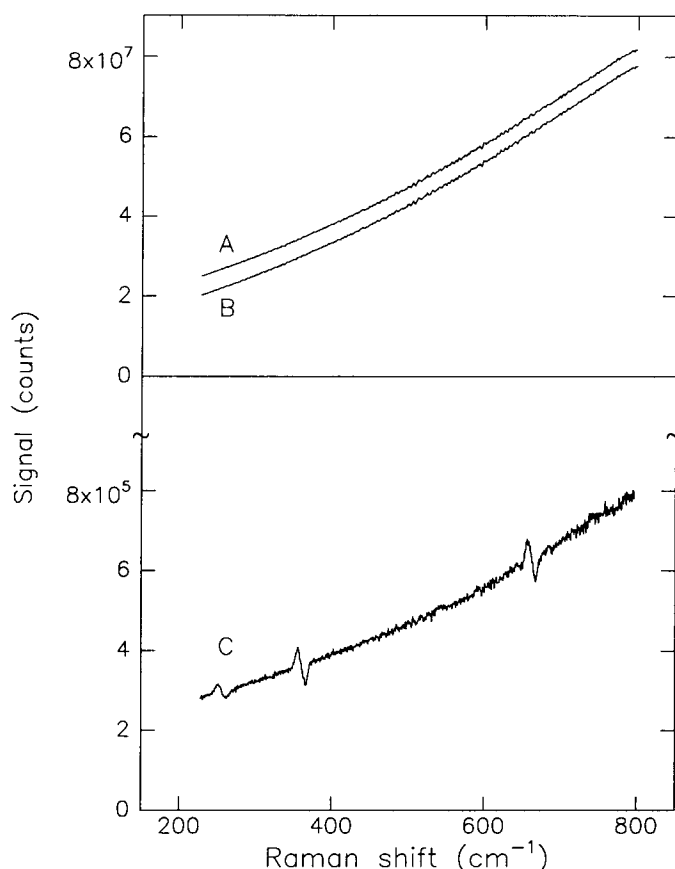


FIG. 2. Curves A and B are emission spectra obtained from the highest dye concentration used ( $\approx 4 \times 10^{-5}$  M). For curve A, the excitation wavelength is 775 nm, while for curve B the excitation is shifted to lower wavelengths by  $10 \text{ cm}^{-1}$ . Curve B is offset by a constant for clarity of presentation. Curve C is the difference of curves A and B ( $B - A$ , with no constant offset). Note that the vertical scales for the two panels differ by a factor of 100.

illustrated. The two curves in the upper panel are spectra obtained at the highest dye concentration shown in Fig. 1. The upper spectrum (A) is obtained with an unshifted laser frequency, while the lower (B) is obtained with the laser frequency shifted by  $10 \text{ cm}^{-1}$  toward lower wavelengths. The lower spectrum has been offset by a constant amount for clarity of presentation. The curve in the lower panel of Fig. 2 (C) is the difference of the shifted and the unshifted curves. Note that the vertical axis in the lower panel is magnified  $100\times$  in comparison to the upper panel. In curve C the features corresponding to the three strong  $\text{CHCl}_3$  Raman lines are clearly observed, even though the Raman peaks are about  $1/1000$  the size of the fluorescence background.

The signal-to-noise ratio in the difference spectrum is consistent with that expected for the shot noise limit. In that limit, the noise for any single spectrum is the square root of the number of counts, and the noise in the difference spectrum is further increased by  $2^{1/2}$ . For a measured spectrum with a large number of counts, one common method to attempt to reach the shot noise limit is to divide the measured spectrum by the spectrum obtained when the detector is illuminated with a spectrally dispersed, broad-band light source. This flat-field correction should serve to remove spectral structure resulting from spatial irregularities in the response of the mul-

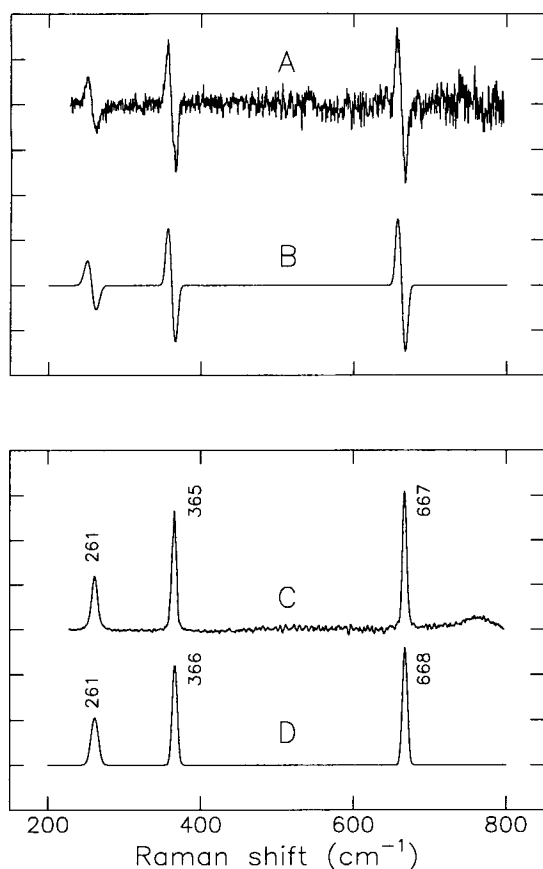


FIG. 3. Spectrum A is the difference spectrum from Fig. 2 with its sloping background removed by a polynomial fit, and curve B is the best fit of Eq. 2 to these data. Spectrum C is the Raman spectrum of the neat  $\text{CHCl}_3$ , and curve D is the spectrum generated from Eq. 1 using the parameters obtained from fitting the difference data (see Table I).

tichannel detector; such irregularities are often as large as several percent of the background signal. However, at large signal levels we have found the shot noise limit difficult to achieve by use of the flat-field correction technique. For example, the spectra in the upper panel of Fig. 2 have been flat-field corrected, but structure is still observed at a level of  $\approx 1/100$  of the signal level, while the shot noise is about  $2 \times 10^{-4}$  times the signal level. Clearly such structure leads to a severe limitation in obtaining Raman spectra by subtraction of a background from flat-field-corrected data; however, the structure is clearly removed in the difference spectrum (lower panel of Fig. 2). Of course, the same difference spectrum is obtained whether the data are flat-field corrected or not, so when the shifted excitation difference technique is used, a flat-field correction is not even necessary.

The generation of a Raman spectrum,  $R(\bar{\nu})$ , from the difference spectrum is shown in Fig. 3. The top spectrum (A) is the difference data from Fig. 2 after subtraction of the small sloping background, while the best fit using  $S(\bar{\nu})$  (Eq. 2) is shown below the data (B). For the fit the number of peaks,  $N$ , is fixed to three. No attempt is made to fit the small feature at  $765 \text{ cm}^{-1}$ . The parameters obtained from the fit to the data are then used in Eq. 1 to generate a Raman spectrum. The lower spectrum of Fig. 3 is the Raman spectrum of neat  $\text{CHCl}_3$  (C; also see the

TABLE I. Comparison of the parameters obtained from modeling the difference spectrum with those obtained from the Raman spectrum of neat  $\text{CHCl}_3$ .

Peak	Difference spectrum model parameters			True spectral parameters		
	Position <sup>a</sup>	Area <sup>b</sup>	FWHM <sup>a,c</sup>	Position <sup>a</sup>	Area <sup>b</sup>	FWHM <sup>a</sup>
1	261	$2.5 \times 10^5$	11	261	$2.5 \times 10^5$	9
2	366	$3.7 \times 10^5$	7	365	$3.6 \times 10^5$	7
3	668	$4.2 \times 10^5$	7	667	$4.7 \times 10^5$	6

<sup>a</sup> In  $\text{cm}^{-1}$ .

<sup>b</sup> Integrated area.

<sup>c</sup> For the Gaussian fit to peak  $i$ , FWHM is  $2\sigma_i(\ln 4)^{1/2}$ .

bottom panel of Fig. 1) and the generated Raman spectrum (D) is shown below the data. In Table I, the peak parameters obtained from fitting the difference data are compared with those obtained directly from the Raman spectrum. As can be seen, the spectrum generated from the difference data agrees well with the known result.

In summary, we have developed a simple method, shifted excitation Raman difference spectroscopy, which is based on taking the difference of two spectra obtained with slightly different excitation wavelengths and which allows Raman lines to be detected even in the presence of a large fluorescence background. As an illustration of the method, Raman scattering from  $\text{CHCl}_3$  in the presence of added fluorescent laser dye has been detected. In this example, Raman peaks that are  $10^{-3}$  times the strength of the fluorescence background are easily observed, even with total data accumulation times for the entire spectrum of only a few minutes. The signal-to-noise is limited by the shot noise of the fluorescence background. Because of the simplicity and effectiveness of the method, we expect that it will see wide applicability in obtaining Raman spectra of fluorescent samples. For example, we have recently used this technique to obtain resonance Raman spectra with excitation directly on resonance with the lowest energy photochemically active absorption band of bacterial photosynthetic reaction centers.<sup>25</sup>

## ACKNOWLEDGMENTS

The idea of using a shifted excitation difference technique to reduce fluorescence interference in Raman spectroscopy was developed through discussions with Tom Middendorf, Stefan Franzen, and Steve Boxer. We thank Phil March and Larry Ynfante of Lexel Laser for arranging the loan of the Ti:sapphire laser used in this work. We also gratefully acknowledge the National Science Foundation, Grant CHE 86-15093, for financial support. A.P.S. is supported by a National Institutes of Health Postdoctoral Fellowship (GM 14298), and N.J.C. acknowledges the Henry Luce Foundation for support by a C. B. Luce Fellowship.

1. J. M. Friedman and R. M. Hochstrasser, *Chem. Phys. Lett.* **33**, 225 (1975).
2. T. Hirschfeld and B. Chase, *Appl. Spectrosc.* **40**, 133 (1986).
3. D. B. Chase, *J. Am. Chem. Soc.* **108**, 7485 (1986).
4. M. Fujiwara, H. Hamaguchi, and M. Tasumi, *Appl. Spectrosc.* **40**, 137 (1986).
5. D. R. Porterfield and A. Campion, *J. Am. Chem. Soc.* **110**, 408 (1988).
6. R. P. Van Duyne, D. L. Jeanmaire, and D. F. Shriver, *Anal. Chem.* **46**, 213 (1974).
7. J. M. Harris, R. W. Chrisman, F. E. Lytle, and R. S. Tobias, *Anal. Chem.* **48**, 1937 (1976).
8. T. L. Gustafson and F. E. Lytle, *Anal. Chem.* **54**, 634 (1982).

9. K. Kamogawa, T. Fujii, and T. Kitagawa, *Appl. Spectrosc.* **42**, 248 (1988).
10. N. Everall, R. W. Jackson, J. Howard, and K. Hutchinson, *J. Raman Spectrosc.* **17**, 415 (1986).
11. J. Howard, N. J. Everall, R. W. Jackson, and K. Hutchinson, *J. Phys. E: Sci. Instrum.* **19**, 934 (1986).
12. S. Burgess and I. W. Shepherd, *J. Phys. E: Sci. Instrum.* **10**, 617 (1977).
13. F. V. Bright and G. M. Hieftje, *Appl. Spectrosc.* **40**, 583 (1986).
14. J. N. Demas and R. A. Keller, *Anal. Chem.* **57**, 538 (1985).
15. A. Z. Genack, *Anal. Chem.* **56**, 2957 (1984).
16. J. Funfschilling and D. F. Williams, *Appl. Spectrosc.* **30**, 443 (1976).
17. F. L. Galeener, *Chem. Phys. Lett.* **48**, 7 (1977).
18. K. H. Levin and C. L. Tang, *Appl. Phys. Lett.* **33**, 817 (1978).
19. S. Brückner, H. Jeziorowski, and H. Knözinger, *Raman Spectroscopy: Linear and Nonlinear*, J. Lascombe and P. V. Huong, Eds. (John Wiley, New York, 1982), p. 253.
20. S. Brückner, H. Jeziorowski and H. Knözinger, *Chem. Phys. Lett.* **105**, 218 (1984).
21. A. B. Myers and R. A. Mathies, in *Biological Applications of Raman Spectrometry*, Vol. 2, T. G. Spiro, Ed. (John Wiley, New York, 1987), p. 1.
22. P. M. Epperson, J. V. Sweedler, R. B. Bilhorn, G. R. Sims, and M. B. Denton, *Anal. Chem.* **60**, 327A (1988).
23. R. Mathies and N.-T. Yu, *J. Raman Spectrosc.* **7**, 349 (1978).
24. J. Laane, in *Vibrational Spectra and Structure*, J. R. Durig, Ed. (Elsevier, Amsterdam, 1983), p. 405.
25. A. P. Shreve, N. J. Cherepy, S. Franzen, S. G. Boxer, and R. A. Mathies, *Proc. Natl. Acad. Sci. (USA)* **88**, 11207 (1991).